Isolated Building Blocks of Photonic Materials: High-Resolution Spectroscopy of Excited States of Jet-Cooled Push-Pull Stilbenes

R. A. Rijkenberg,[†] D. Bebelaar,[†] W. J. Buma,*[,†] and J. W. Hofstraat[‡]

Faculty of Science, Institute of Molecular Chemistry, University of Amsterdam, Nieuwe Achtergracht 127−129, 1018 WS Amsterdam, The Netherlands, and Department of Polymers and Organic Chemistry, Philips Research, Prof. Holstlaan 4 (WB63), 5656 AA Eindhoven, The Netherlands

Received: September 6, 2001; In Final Form: November 20, 2001

The lowest excited singlet states of 4-(dimethylamino)-4′-cyanostilbene (DCS), 4-(dimethylamino)-4′-nitrostilbene (DANS), and 4-di(hydroxy-ethyl)amino-4′-nitrostilbene (DANS-diol) have been investigated by high-resolution fluorescence excitation and dispersed emission spectroscopy on samples seeded in supersonic expansions. Using ab initio calculations of the harmonic force fields of the electronic ground state as a starting point for the analysis of vibrational modes and frequencies, detailed vibrational assignments of the rich line structure of the $S_1 \leftarrow S_0$ transition in these three push−pull stilbenes are reported. From the experimental and theoretical analysis, it becomes apparent that the excitation spectra are dominated by low-frequency vibrational modes of the stilbene-like backbone, albeit that a characterization in terms of *trans*-stilbene vibrational terminology is not very appropriate. The fluorescence excitation and emission spectra show significant Franck−Condon factors for transitions involving these vibrational modes, in line with significant geometry changes in the stilbene moiety upon electronic excitation. Comparison of the spectroscopic data of the DANS chromophore in DANS and DANS-diol demonstrates that the inclusion of the diol auxiliary function has a significant effect on its spectroscopic properties. Similarly, the comparison between solution and gas-phase data leads to the conclusion that spectroscopic data obtained in solution for DCS allow for a reasonably good extrapolation to the isolated molecule but that the structure of DANS is, even in low-polarity solvents, already modified to a larger extent than would a priori be expected.

I. Introduction

Push−pull stilbenes are highly prominent candidates for building blocks for future nonlinear photonic materials because of their high second- and third-order polarizabilities.[1−3] The tailorability of these organic conjugated push−pull molecules allows one to customize the chemical structure and their properties for specific technological applications,[1,4−6] such as electrooptic and frequency-doubling devices. For the development of new materials with improved − and ultimately user-defined − photoresponsive properties, it is essential to understand the relevant photophysics and photochemistry of the systems at the molecular level.[1−12]

Not surprisingly, considerable research has therefore been dedicated to elucidate the spectroscopic and dynamic properties of these push−pull stilbenes, albeit that the vast majority of these studies has been performed in solution. Primary targets of these studies have been 4-(dimethylamino)-4′-cyanostilbene (DCS)[13−26] and 4-(dimethylamino)-4′-nitrostilbene (DANS)[26−36] (see Figure 1), with as a goal to investigate and understand their photophysics and photochemistry, in particular in relation to the intramolecular charge transfer (ICT) process that leads to sudden polarization[37−40] upon excitation from the electronic ground state to the equilibrated singlet excited state. Various theoretical and experimental studies have given evidence for and corroborated the presence of sudden polarization in DCS and DANS upon excitation.[2,3,26,35,41−48]

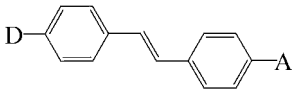

DCS:	$D = N(CH_3)_2$	$A = CN$
DANS:	$D = N(CH_3)_2$	$A = NO_2$
DANS-diol:	$D = N(CH_2CH_2OH)_2$	$A = NO_2$

Figure 1. Molecular structures of the targeted push−pull stilbenes: 4-(dimethylamino)-4′-cyanostilbene (DCS), 4-(dimethylamino)-4′-nitrostilbene (DANS), and 4-di(hydroxy-ethyl)amino-4′-nitrostilbene (DANS-diol).

Femtosecond fluorescence spectroscopy on DCS in polar solutions has shown a fast and efficient ICT process occurring on a time scale of the order of one picosecond.[23,24] Analysis of the solvatochromic shift of the absorption maxima as a function of the solvent polarity provided experimental evidence that in DCS the locally excited (LE) state has a dipole moment of 13 D,[24] giving reason to believe that even this state has already to a large extent CT character.[23,24] This was supported by a recent ab initio CI study on DCS,[48] which showed that the LE state is mainly described by a single excitation from the highest occupied molecular orbital (HOMO), localized to a large extent on the dimethylanilino group and the linkage ethylenic part, to the lowest unoccupied molecular orbital (LUMO), localized primarily on the 4-cyanostyryl group. In polar solvents, a second state of CT character becomes sufficiently stabilized to be accessible, giving rise to the sudden polarization effect.[14−16,18,19,24,25] Experimental studies investigating selectively bridged derivatives of DCS suggest that this CT state, also referred to as a twisted intramolecular CT (TICT) state, is

* To whom correspondence should be addressed. E-mail: wybren@fys.chem.uva.nl. Fax: (31)-20−525 6456/6422.
[†] University of Amsterdam.
[‡] Philips Research.

10.1021/jp013422j CCC: $22.00
Published on Web 02/14/2002

coupled to the initially prepared LE state via a normal coordinate associated with a rotation around the bond linking the dimethyl-anilino group to the double bond.[14−16,18,19,25] The dependence of the solvatochromic shift of the emission maxima on the solvent polarity[24] has been interpreted to indicate that this twisting motion, which leads to strongly enhanced charge-transfer, is responsible for the sudden polarization phenomenon and results in a further increase of the dipole moment of DCS in this TICT state by roughly 9 D. Recent ab initio configuration interaction (CI) calculations on the electronic properties of the lowest excited singlet state of DCS under both isolated conditions and in a polar environment corroborate these experimental observations.[48]

Because of the large difference in acceptor strength of the nitro group as compared to that of the cyano group, the same phenomena, and probably even magnified, can be expected for DANS.[26] Indeed, experimental studies[35,42,43] show that the dipole moment of DANS in its LE state is about 23 D, implying a dramatic increase of 16 D upon photoexcitation. This experimental value is close to the ab initio value of 22 D calculated by Brédas et al.[2,3] for the dipole moment μ_e of the LE state. Lapouyade et al.[26] determined the dipole moment of the CT state in DANS using the solvatochromic shift of the emission maxima in a number of polar solvents and reported a dipole moment μ_e of the equilibrated singlet excited state of about 42 D. This suggests that the dipole moment of the singlet excited state increases by another 19 D in the evolution from the LE to the CT state. Such an increase is significantly larger than what is observed for DCS and is supported by CNDO/S calculations[26] of the dipole moment of DANS in its equilibrated singlet excited state in polar solvents. The qualitative picture that arises from this CNDO/S study is that both DCS and DANS will show strongly enhanced charge-transfer upon a twisting motion around the bond linking the dimethyl-anilino group to the double bond.

The strong and efficient ICT process occurring in these compounds may lead to a significant enhancement of the second- and third-order optical response.[1−12] Several studies have therefore investigated the nonlinear optical response, focusing on DANS as a benchmark system.[2,3,49] In a joint theoretical and experimental study on the nonlinear optical response of DANS,[2] it was concluded that an appropriate theoretical model describing this response requires an accurate description of both the electronic and vibronic structures of the lowest singlet excited states. To gain full insight into the electronic and vibronic structures of these push−pull stilbenes, as well as the role played by intermolecular interactions in solution and the solid state, studies of their spectroscopic properties under isolated conditions are crucial. Only in this way, a full appreciation of the intra- and intermolecular interactions governing their nonlinear optical properties is obtained. In this spirit, we have first applied low-resolution spectroscopy on substituted stilbenes vapor to establish the approximate spectral domain of the $S_1 \leftarrow S_0$ transition in the isolated molecules and subsequently performed high-resolution fluorescence excitation and dispersed emission spectroscopy on jet-cooled push−pull stilbenes.

As yet, experimental studies of the spectroscopic properties of such molecules under isolated conditions have been limited to one fluorescence study of jet-cooled DCS.[50] In that study, the main features of the fluorescence excitation and dispersed emission spectrum of the lowest singlet excited state were addressed, but the main focus was on the *dynamics* of the lowest singlet excited state. In the present study, we will go into significantly more depth with respect to the *spectroscopic* properties of push−pull stilbenes. As targets for this investigation, DCS and DANS have been selected. To start to understand the influence of intra- and intermolecular interactions on the spectroscopic properties of such molecules, we have also studied a chemically modified DANS chromophore (see Figure 1), 4-di-(hydroxy-ethyl)amino-4′-nitrostilbene (DANS-diol), which is normally used to incorporate DANS as a side group in a side-chain polymer.[1] The role of intermolecular interactions will be discussed by comparing the present data obtained for the isolated chromophores with results previously obtained in solution.

II. Experimental and Theoretical Details

A. Experimental Procedures. Details of the setups used to perform fluorescence excitation and dispersed emission spectroscopy on (i) heated samples of DCS, DANS, and DANS-diol in quartz cells[51] and (ii) compounds seeded in a continuous or pulsed supersonic expansion[52,53] have been reported elsewhere. Briefly, low-resolution fluorescence excitation and emission spectra were obtained using a SPEX Fluorolog 2 instrument equipped with a red-sensitive GaAs photomultiplier (RCA-C31034, Peltier cooled) for which the spectral response extends to $\leq$900 nm and is known to be quite flat from the UV to about 860 nm. In these experiments, samples were placed in a quartz cell (10 × 10 mm) suitable for high temperature measurements, which was successively sealed by fusing the graded seals and leaving the sample in a vacuum environment. The cells were placed in an oven with quartz windows at right angles and heated to about 550 K in order to obtain sufficient vapor pressure for the measurements.

High-resolution fluorescence excitation and dispersed emission fluorescence spectra were obtained using a setup in which excitation is achieved by a dye laser (Lumonics HyperDye-300) pumped by a XeCl excimer laser (Lambda Physik EMG103MSC) and operating on the laser dyes DMQ, RDC 360, Exalite 351, PTP, or DCM. In the case of DCM, the output of the dye laser was frequency-doubled by an angle-tuned KDP crystal in an Inrad Autotracker II unit. The fundamental dye laser light has a spectral bandwidth of about 0.07 cm^{-1} and a pulse duration of about 15 ns. Calibration of the wavelength of the dye laser output was achieved by using the optogalvanic spectrum of Ne excited in a hollow-cathode discharge. The intensity of the dye laser beam was monitored by measuring its intensity with an EG&G radiometer model 580, which was read out by a computer controlling the experiment.

The excitation beam was steered into the vacuum chamber, where it crossed at right angles a supersonic expansion. This expansion was generated by heating the sample to temperatures ranging from 440 up to 490 K, seeding the vapor into 3 bar of He, and expanding it into a vacuum chamber via a pulsed valve with a 500 μm diameter orifice (General Valve Iota One System). The coil assembly is equipped with a "hot-body coil" (General Valve Series 9) to allow for temperatures up to 508 K. Optimal time overlap between the pulsed molecular beam and the laser pulse was achieved using a homemade delay generator. Fluorescence from the jet-cooled compounds was collected at right angles with respect to the excitation light and the molecular beam by a spherical quartz condenser (Melles Griot 01MCP119; diameter 50 mm, focal length 50 mm) and imaged onto the slit of a Zeiss M20 grating monochromator equipped with an EMI 9558 QA (S20) photomultiplier.

In the fluorescence excitation experiments, the monochromator was used with a slit width of 8 mm, resulting in a spectral resolution of 40 nm. Centre emission wavelengths of 400, 390, and 390 nm were employed for DCS, DANS, and DANS-diol, respectively. The output of the photomultiplier was integrated

with a boxcar integrator (SR250), whose output was read out and averaged by the computer. In a typical experiment, excitation spectra were obtained by scanning the dye laser in steps of 0.05 cm^{-1}, averaging over 30 laser pulses, and dividing the fluorescence signal by the laser intensity as measured by the radiometer. For DCS and DANS, single level dispersed emission spectra have been recorded as well. In these experiments, the photomultiplier was cooled with a mixture of ethanol and dry ice (−78 °C) to reduce its dark current. Emission spectra were obtained by scanning the monochromator with a slit width of 0.1 mm (spectral resolution of about 40 cm^{-1}) and averaging the signal over 60 and 150 laser pulses for DCS and DANS, respectively.

B. Theoretical Procedures. Calculations on the electronic ground states of *trans*-stilbene, DCS, and DANS have been performed using the Gaussian 98 suite of programs.[54] Optimized geometries and harmonic force fields were obtained using the hybrid density functional B3LYP[55] methods with the 6-31G* basis set.

III. Results and Discussion

In the following, the fluorescence excitation and emission spectra of jet-cooled DCS, DANS, and DANS-diol will be presented and discussed (sections B−D). Previous studies on high-resolution spectra of substituted stilbenes[56−59] have demonstrated that in these spectra a plethora of vibronic transitions can be expected to be difficult to assign from first principles. In fact, dominant peaks in these spectra have in the past generally been assigned by looking at the active modes in the analogous spectra of the unsubstituted *trans*-stilbene molecule.[60−64] Although as an initial attempt this approach is of course reasonable, and also followed by us, it is at the same time clear that normal modes in the substituted stilbenes can be heavily affected in frequency and atomic displacements by the substituents, making it questionable whether the use of stilbene vibrational labels is always valid. To put the present assignments on a somewhat firmer ground, and to get a grasp on the extent to which the substituted stilbene spectra can be compared with those of *trans*-stilbene, we have performed ab initio B3LYP/6-31G* calculations of the equilibrium geometry and associated harmonic force fields of DCS and DANS in their electronic ground states. Although the ground-state frequencies are different from those of the excited state, they should give a good indication of where to expect vibronic transitions in the excitation spectrum. To enable a valid comparison, calculations at the same level have been performed on the ground state of *trans*-stilbene as well. These results will be presented and discussed in section A.

The analysis of the excitation and emission spectra is intended to elucidate the electronic properties of the molecules under isolated conditions. However, in technological applications, the substituted stilbenes are employed under nonisolated conditions. The results obtained under isolated conditions will consequently be used to investigate the role of intermolecular interactions by comparison of the spectroscopic properties of isolated and solvated DCS and DANS (section E). This comparison will show an unexpected influence of solute−solvent interactions for solvents that are normally assumed to exert negligible influence on the spectroscopic properties of the types of molecules considered here.

A. Ab Initio Calculations. Although previously the subject of extensive discussion, recent high-resolution spectroscopic studies have by now firmly established that *trans*-stilbene is planar in the electronic ground state and remains planar upon excitation to its first excited state.[60,65] We have therefore performed our calculations under the restriction of C_s symmetry for the substituted stilbenes, and C_{2h} symmetry for *trans*-stilbene. Geometry optimization and the subsequent calculation of the harmonic force fields then leads to the frequencies reported in Table 1 for the three molecules. This table also contains a description of the modes in the substituted stilbenes in terms of vibrational modes in *trans*-stilbene as obtained by visual inspection. We explicitly notice that such a description is per se only very approximate: its only use is to indicate the parental vibrational motion of the *trans*-stilbene skeleton, with in the back of our mind the thought that active modes in the spectra of *trans*-stilbene might also show activity in these substituted stilbene modes. As expected, the DCS and DANS vibrational modes are on the other hand very similar. Some vibrational modes of DANS that do not have a counterpart in DCS have not been included in the table. Because the excitation spectra do not show transitions about 1200 cm^{-1} above the 0−0 transition, only the *in-plane* modes (of a′ symmetry for DCS and DANS and of a_g or b_u symmetry for *trans*-stilbene) with frequencies of up to about 1200 cm^{-1} are included in Table 1. Additionally, Table 1 contains the lower-frequency *out-of-plane* modes (of a_u and b_g symmetry in *trans*-stilbene and of a″ symmetry in DCS and DANS) of which activity has previously been invoked in the excitation and emission spectra of *trans*-stilbene.[60−64] With respect to these out-of-plane modes, some caution should be taken. First, in *trans*-stilbene, ν_{37} changes considerably in frequency upon excitation (roughly from 8 to 48 cm^{-1} [60]). A similar change can be anticipated for the

TABLE 1: Calculated B3LYP/6-31G* Ground State Frequencies (cm^{-1}) for Relevant Vibrational Modes of DCS and DANS and the *trans*-Stilbene Parentage[a]

	DCS	DANS	description
		In-Plane Modes	
a′(1)	48	47	ν_{72} (b_u) (*80*)
a′(2)	131	142	ν_{25} (a_g) (*207*)
a′(3)	176	189	ν_{25} (a_g) (*207*)
a′(4)	213	252	ν_{24} (a_g) (*288*)
a′(5)	296	320	ν_{24} (a_g) (*288*)
a′(6)	389	373	local mode
a′(7)	449	455	ν_{71} (b_u) (*473*)
a′(8)	480	443	ν_{70} (b_u) (*551*) + local mode
a′(9)	505	503	ν_{71} (b_u) (*473*)
a′(10)	561	536	local mode
a′(11)	572	544	local mode
a′(12)	654	646	ν_{23} (a_g) (*633*)
a′(13)	664	657	ν_{69} (b_u) (*637*)
a′(14)	726	675	ν_{70} (b_u) (*551*) + local mode
a′(15)	763	738	ν_{22} (a_g) (*655*)
a′(16)	850	867	ν_{68} (b_u) (*837*)
a′(17)	892	895	ν_{21} (a_g) (*887*)
a′(18)	972	972	local mode
a′(19)	1023	1022	ν_{19} (a_g) (*1058*) ±
a′(20)	1034	1029	ν_{66} (b_u) (*1060*)
a′(21)	1092	1095	local mode
a′(22)	1149	1141	ν_{18} (a_g) (*1116*) ±
a′(23)	1168	1169	ν_{65} (b_u) (*1113*)
		Out-of-Plane Modes	
a″(1)	37i	168i	local mode
a″(2)	16	8	ν_{37} (a_u) (*7i*)
a″(3)	29	27	ν_{36} (a_u) (*59*)
a″(4)	59	56	ν_{48} (b_g) (*62*)
a″(5)	72	75i	local mode

[a] Calculated frequencies (cm^{-1}) of *trans*-stilbene modes referred to are given in italics in parentheses.

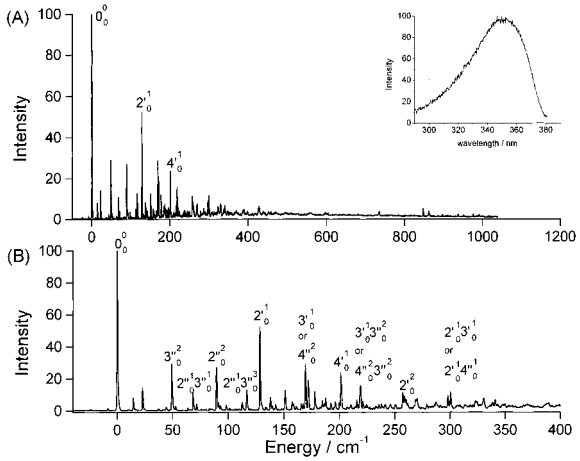

Figure 2. Fluorescence excitation spectrum of the $S_1 \leftarrow S_0$ transition of jet-cooled DCS. The excitation energy is given with respect to the 0−0 transition located at 27 061.9 cm^{-1}. (A) Overall $S_1 \leftarrow S_0$ excitation spectrum. The inset displays the excitation spectrum of DCS vapor at 550 K. (B) Expanded view of the 0−400 cm^{-1} region.

substituted stilbenes. Second, for ν_{48} (b_g) of *trans*-stilbene, a frequency of 62 cm^{-1} is calculated, whereas the experimental frequency is 132 cm^{-1}.[66] Other calculations[67−69] indeed find a much larger frequency than what the B3LYP/6-31G* calculation gives. The reason for this difference is not clear.

Table 1 shows that the symmetry restrictions give rise to a number of imaginary frequencies. In the case of *trans*-stilbene, the associated mode is the out-of-plane phenyl torsion ν_{37}. The study of Choi and Kertesz[67] has shown that allowing a lowering of the symmetry at the B3LYP/6-31G* level leads only to a minor out-of-plane distortion: a dihedral angle of 0.1° was reported. For DCS, the imaginary frequency is associated with the dimethylamino inversion mode, and for DANS, the two frequencies concern a dimethylamino rotation−inversion mode (168i cm^{-1}) and a methyl rotation mode (75i cm^{-1}). In all cases, deformation of the molecules along the modes with an imaginary frequency is in first order not expected to influence the form and frequencies of the in-plane modes, which are the ones for which vibrational activity resulting from geometry changes upon excitation may be expected, and we will therefore assume that it is valid to take the atomic displacements and frequencies of the normal modes given in Table 1 as a guide for further analysis.

As was suspected already, Table 1 confirms that the absence of a clear one-to-one correspondence between substituted stilbene and *trans*-stilbene modes is more the rule than the exception. On the basis of vibrational activity in the *trans*-stilbene excitation and emission spectra,[60−64] we may therefore anticipate a considerable increase of vibrational activity in the substituted stilbene spectra.

B. 4-(Dimethylamino)-4′-cyanostilbene (DCS). The one-photon fluorescence excitation spectrum of the $S_1(2^1A') \leftarrow S_0$-$(1^1A')$ transition of DCS, heated to 440 K and seeded in a supersonic jet expansion of He, is shown in Figure 2. Overall, the spectrum is in good agreement with the jet-cooled spectrum of Daum et al.,[50] although the spectra differ in two aspects. First, in the present study, the 0−0 transition is found at 27 061.9 cm^{-1}, whereas previously, a value of 27 038 cm^{-1} was reported. Second, the intensity of transitions roughly 200 cm^{-1} above the 0−0 transition is significantly lower in the present study, possibly because of saturation effects in the previous study. The inset of Figure 2 displays the fluorescence excitation spectrum of DCS vapor at about 550 K in a heated quartz cell. Under these conditions, the maximum fluorescence intensity is obtained by excitation with 352 nm (∼28 410 cm^{-1}). In agreement with general experience, our experimental value of 3.52 eV for the vertical excitation energy of the $S_1 \leftarrow S_0$ transition is about 0.3 eV lower than what previous semiempirical studies have predicted.[17,25,26]

The jet-cooled spectrum displayed in Figure 2 exhibits a rich and pronounced vibrational line structure up to 500 cm^{-1} above the 0−0 transition. As will be argued below, these transitions can be assigned in terms of principally low-frequency vibrational modes of the stilbene-like backbone of DCS. Above this energy, the vibrational activity decreases rapidly and only a few pronounced features can be discerned. The present study confirms for the majority of the bands the assignments as proposed by Daum et al.[50] but at the same time assigns considerably more bands (see Table 2). Excited state frequencies of optically active modes derived from these assignments are given in Table 3. For totally symmetric modes, these frequencies are taken as the $(\nu_i)_0^1$ transition energies, and for nontotally symmetric modes, half of the $(\nu_i)_0^2$ transition energy is reported.

The most intense line in the excitation spectrum of *trans*-stilbene appears at 198 cm^{-1} and has been assigned to the 25_0^1 transition, with 25_0^2 and 25_0^3 overtone transitions occurring at 396 and 594 cm^{-1}.[64] Table 1 shows then that the lines at 128.2 and 257.0 cm^{-1} in the excitation spectrum of DCS are most readily assigned to the $a'(2)_0^1$ transition and its first overtone. This assignment is in agreement with previous assignments[50] and assignments of the "25_0^1" transition in other jet-cooled substituted stilbenes.[56−59] Chiang and Laane[62] recently proposed the alternative assignments 35_0^2 and 35_0^4 for the 198 and 396 cm^{-1} lines in *trans*-stilbene. Apart from the arguments put forward in the analysis of excitation spectra of other substituted stilbenes,[57] namely, that the intensity of the bands is too large to account for on the basis of frequency differences in ground and excited states, the dispersed emission spectrum and photoionization behavior after excitation of this level,[61,64] as well as the extensive ab initio calculations on *trans*-stilbene of Choi and Kertesz,[67] lead to disagreement with such a conclusion. We therefore adhere to the original assignment. Having concluded that the ν_{25} activity of *trans*-stilbene is transferred to the substituted stilbenes and seeing that a′(3) has also considerable ν_{25} parentage, it is most logical to assign either the 169.1 or 171.7 cm^{-1} line to the $a'(3)_0^1$ transition.

In the excitation spectrum of *trans*-stilbene, the strong 24_0^1 transition occurs at 280 cm^{-1}.[64] On the basis of its activity, the strong band observed for DCS at 201.2 cm^{-1} is assigned to the $a'(4)_0^1$ transition. Considering that a′(5) is also of ν_{24} parentage would make us expect around 290 cm^{-1} the $a'(5)_0^1$ transition. Although there is more than enough vibrational activity in this region, there is not one particular resonance that might unambiguously be assigned as $a'(5)_0^1$.

The fluorescence excitation spectrum of DCS shows two prominent lines at 49.2 and 89.4 cm^{-1}, which we assign as the $a''(3)_0^2$ and $a''(2)_0^2$ transitions, respectively. Spangler et al.[57] have argued that *para* substitution of *trans*-stilbene should have a large effect on the ν_{36} asymmetric phenyl flap mode because of a large increase of the reduced mass, whereas the ν_{37} ring torsion mode should only be marginally affected as the substituents lie on the torsional axis and hardly contribute to the reduced moment of inertia. In *trans*-stilbene, the 36_0^2 and 37_0^2 transitions occur at 69.6 and 95.3 cm^{-1}, respectively.[60] The observed shifts of −20.4 and −6.1 cm^{-1}, respectively, thus

TABLE 2: Assignments of the Vibronic Transitions in the $S_1(2^1A')$ ← $S_0(1^1A')$ Fluorescence Excitation Spectrum of Jet-Cooled DCS

energy	intensity	assignment	energy	intensity	assignment
0	100	0_0^0	288.7	2	$3'_0{}^1 2''_0{}^1 3''_0{}^3$ or $4''_0{}^2 2''_0{}^1 3''_0{}^3$
49.2	26	$3''_0{}^2$	290.8	2	$4'_0{}^1 2''_0{}^2$
68.3	11	$2''_0{}^1 3''_0{}^1$	297.9	6	$2'_0{}^1 3'_0{}^1$ or $2'_0{}^1 4''_0{}^2$
			300.2	10	
89.4	17	$2''_0{}^2$	306.5	2	$2'_0{}^1 2''_0{}^4$
98.0	3	$3''_0{}^4$	330.0	5	$2'_0{}^1 4'_0{}^1$
116.7	10	$2''_0{}^1 3''_0{}^3$	338.6	3	$3'_0{}^2$ or $4''_0{}^4$
128.2	49	$2'_0{}^1$	340.8	4	$3'_0{}^1 4''_0{}^2$
129.9	23	$4''_0{}^1 2''_0{}^1$	343.0	2	$3'_0{}^2$ or $4''_0{}^4$
137.9	4	$2''_0{}^2 3''_0{}^2$	349.3	3	$3'_0{}^1 2''_0{}^4$ or $4''_0{}^2 2''_0{}^4$
157.1	4	$2''_0{}^3 3''_0{}^1$	428.4	4	$2'_0{}^2 3'_0{}^1$ or $2'_0{}^2 4''_0{}^2$
167.1	4	$2''_0{}^1 3''_0{}^5$			
169.1	27	$3'_0{}^1$ or $4''_0{}^2$	597.6	1	$12'_0{}^1$
171.7	19		603.9	1	$13'_0{}^1$
177.5	12	$2'_0{}^1 3''_0{}^2$	735.2	2	$15'_0{}^1$
187.3	7	$3''_0{}^4 2''_0{}^2$	784.1	1	$15'_0{}^1 3''_0{}^2$
196.2	5	$2'_0{}^1 2''_0{}^1 3''_0{}^1$	824.3	1	$15'_0{}^1 2''_0{}^2$
201.2	22	$4'_0{}^1$	847.3	4	$16'_0{}^1$
207.0	2	$2''_0{}^3 3''_0{}^3$	861.6	3	$17'_0{}^1$
218.5	12	$3'_0{}^1 3''_0{}^2$ or $4''_0{}^2 3''_0{}^2$	863.6	1	$2'_0{}^1 15'_0{}^1$
220.9	4				
237.8	3	$3'_0{}^1 2''_0{}^1 3''_0{}^1$ or $4''_0{}^2 2''_0{}^1 3''_0{}^1$	896.4	1	$16'_0{}^1 3''_0{}^2$
240.5	2		910.5	1	$17'_0{}^1 3''_0{}^2$
250.4	3	$4'_0{}^1 3''_0{}^2$	937.1	1	$16'_0{}^1 2''_0{}^2$
257.0	11	$2'_0{}^2$	951.0	1	$17'_0{}^1 2''_0{}^2$
258.5	8	$3'_0{}^1 2''_0{}^2$ or $4''_0{}^2 2''_0{}^2$	976.0	1	$2'_0{}^1 16'_0{}^1$
259.9	6		989.9	1	$2'_0{}^1 17'_0{}^1$
267.5	2	$2''_0{}^6$	1017.0	1	$19'_0{}^1$ or $20'_0{}^1$
269.5	5	$3'_0{}^1 3''_0{}^4$ or $4''_0{}^2 3''_0{}^4$	976.0	1	$2'_0{}^1 16'_0{}^1$
270.0	6	$4'_0{}^1 2''_0{}^1 3''_0{}^1$	989.9	1	$2'_0{}^1 17'_0{}^1$
285.9	3	$2'_0{}^1 2''_0{}^3 3''_0{}^1$	1017.0	1	$19'_0{}^1$ or $20'_0{}^1$

TABLE 3: Experimental Excited State Frequencies (cm^{-1}) Determined from the $S_1(2^1A')$ ← $S_0(1^1A')$ Fluorescence Excitation Spectra of DCS, DANS, and DANS-diol[a]

mode	DCS	DANS	DANS-diol	description
		In-Plane Modes		
a′(2)	128.2	155.1	176.4	ν_{25} (a_g) (*207*)
a′(3)	∼170			ν_{25} (a_g) (*207*)
a′(4)	201.2	205.5	245.2	ν_{24} (a_g) (*288*)
a′(12)	597.6	593.4		ν_{23} (a_g) (*633*)
a′(13)	603.9	615.3		ν_{69} (b_u) (*637*)
a′(15)	735.2	736.7		ν_{22} (a_g) (*655*)
a′(16)	847.3			ν_{68} (b_u) (*837*)
a′(17)	861.6			ν_{21} (a_g) (*887*)
a′(19)	1017			ν_{19} (a_g) (*1058*) ±
a′(20)	1017			ν_{66} (b_u) (*1060*)
		Out-of-Plane Modes		
a″(2)	44.7	52.7	49.6	ν_{37} (a_u) (*7i*)
a″(3)	24.6	24.6	19.3	ν_{36} (a_u) (*59*)
a″(4)	∼170			ν_{48} (b_g) (*62*)

[a] Calculated frequencies (cm^{-1}) of *trans*-stilbene modes referred to are given in italics in parentheses.

support our assignment in DCS and are consistent with similar observations obtained for methyl-substituted stilbenes[56] as well as other more heavily substituted stilbenes.[57−59] The strong feature at 68.3 cm^{-1}, which can be assigned to the $a''(2)_0^1 a''(3)_0^1$ transition, provides further support for these assignments. The assignment of the $a''(2)_0^2$ transition agrees with the conclusions of Daum et al.[50] They assign the $a''(3)_0^2$ transition, however, to a resonance at 42.5 cm^{-1} that appears only as a very weak line in the fluorescence excitation spectrum and suggest that the resonance at 49.2 cm^{-1} corresponds to ring motions on a torsional potential energy surface modified by the presence of the cyano and dimethylamino groups.

Daum et al.[50] discussed the fluorescence excitation spectrum of isolated DCS not only in terms of the low-frequency vibrational modes of *trans*-stilbene but considered some six lines to be associated with rotation and inversion modes of the dimethylamino group. For these assignments, they referred to a spectroscopic study by Grassian et al.[70] on the rotational and inversion motions of the dimethylamino group in substituted dimethylaminobenzenes. However, in these molecules a considerable reorientation of the dimethylamino group occurs upon excitation, as a result of which the excitation spectrum of those molecules displays a very weak 0−0 transition, and extended activity in the mentioned modes. In DCS, in contrast, the 0−0 transition is the strongest transition, and the resonances supposedly associated with the rotation and inversion modes are very much weaker. This would not be in line with Franck−Condon intensity expectations.

The "high-energy" region of the fluorescence excitation spectrum of DCS shows a number of features that on the basis of their intensity and/or frequency cannot be assigned as combination bands. In particular, the resonances at 597.6, 603.9, 735.2, 847.3, 861.6, and 1017.0 cm^{-1} are tentatively assigned using Table 1 as fundamentals of vibrational modes located primarily on the stilbene-like backbone of DCS. They correspond to the $a'(12)_0^1$, $a'(13)_0^1$, $a'(15)_0^1$, $a'(16)_0^1$, $a'(17)_0^1$, and $a'(19)_0^1$ or $a'(20)_0^1$ transitions associated with the ν_{23}, ν_{67}, ν_{22}, ν_{68}, ν_{21}, and ν_{19} modes, respectively, of *trans*-stilbene. The 735.2, 847.3, and 861.6 cm^{-1} modes give rise to combination bands with other, low-frequency, modes.

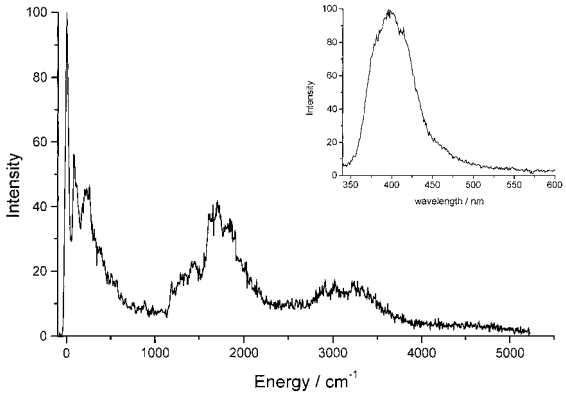

Figure 3. Emission spectrum of jet-cooled DCS excited at the 0−0 transition (27 061.9 cm^{-1}) to the first excited singlet state. Fluorescence wavelengths are given as shifts from the excitation wavelength. The inset displays the emission spectrum of DCS vapor at 550 K (λ_{exc}=340 nm).

The two strong lines at 14.5 and 22.8 cm^{-1} have previously[50] not been discussed yet seem to play a pivotal role in the fluorescence excitation spectrum of jet-cooled DCS. Many features in the spectrum can be readily assigned as combination bands of these two features with other, low-frequency, vibrational modes. Table 1 clearly indicates, however, that these features cannot be associated with totally symmetric vibrations. Comparison of our spectrum with the spectrum in ref 50 demonstrates that the intensities of the two bands are rather dependent on the expansion conditions. This would argue for their assignment as hot band transitions that most probably involve the a″(2) and a″(3) modes associated with the ν_{36} and ν_{37} modes in *trans*-stilbene.

One final resonance that merits further discussion concerns the remaining resonance of the pair at 169.1 or 171.7 cm^{-1}. One of these two, although it is not clear which one, has been assigned to the $a'(3)_0^1$ transition (vide supra), but what about the remaining one? In fluorescence excitation studies of *p*-methyl-*trans*-stilbene,[56] *syn*- and *anti*-p-hydroxy-p′-methyl-*trans*-stilbene,[59] and p-methoxy-*trans*-stilbene[58] a similar resonance was observed at 191, (154 and 169), and 161 cm^{-1}, respectively. In these studies, a 72_0^1 (the lowest-frequency b_u mode of *trans*-stilbene predicted at 60−80 cm^{-1}) assignment was tentatively put forward. Our calculations (see Table 1) do not support such an assignment; they predict that the frequency of the analogous mode in the substituted stilbenes *decreases* instead of being more than 2-fold *increased*. With the totally symmetric vibrations having been exhausted, one of the few possibilities that remain is the $a''(4)_0^2$ transition, associated with the 48_0^2 transition of *trans*-stilbene. Above we noticed that the B3LYP functional performs rather badly for ν_{48}: a frequency of 62 cm^{-1} was predicted for *trans*-stilbene, instead of a value around 130 cm^{-1}.[66] We assume that the same happens for DCS and DANS, explaining the apparent mismatch between the experimentally observed and theoretically predicted frequency.

The dispersed fluorescence emission spectrum obtained after excitation at the 0−0 transition to S_1 of jet-cooled DCS, heated to 470 K and seeded in a supersonic jet expansion of He, is displayed in Figure 3. It is in excellent agreement with that obtained by Daum et al.[50] However, because of the lack in detail in this spectrum resulting from a poorer resolution, we will only present the spectrum for the sake of completeness and omit any detailed assignment of the features. What is clear and of importance for further considerations of geometry displacements between ground and excited state (vide infra), is that modes

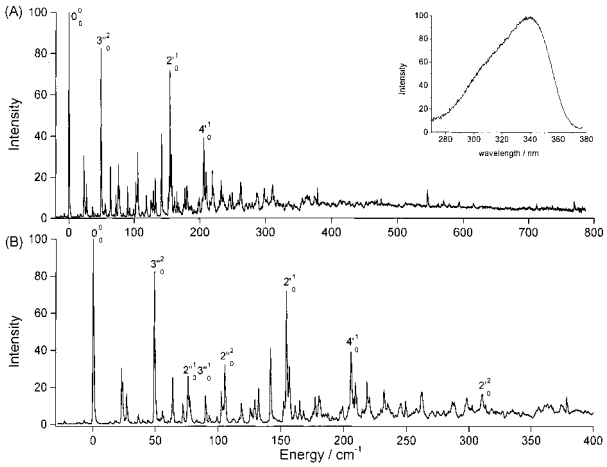

Figure 4. Fluorescence excitation spectrum of the $S_1 \leftarrow S_0$ transition of jet-cooled DANS. The excitation energy is given with respect to the energy of the 0−0 transition located at 28 200.1 cm^{-1}. (A) Overall $S_1 \leftarrow S_0$ excitation spectrum. The inset displays the excitation spectrum of DANS vapor at 550 K. (B) Expanded view of the 0−400 cm^{-1} region.

around 150, 1200−1300, and 1600 cm^{-1} play an important role. The inset of this figure shows the low-resolution fluorescence emission spectrum of DCS vapor in a quartz cell at 550 K. In this case, the maximum fluorescence intensity is collected at 402 nm (∼24876 cm^{-1}).

C. 4-(Dimethylamino)-4′-nitrostilbene (DANS). Figure 4 shows the fluorescence excitation spectrum of the $S_1(2^1A') \leftarrow S_0(1^1A')$ transition of jet-cooled DANS, heated to 470 K and seeded in an expansion of He. The 0−0 transition is observed at 28 200.1 cm^{-1}. The inset of Figure 4 shows the low-resolution fluorescence excitation spectrum of DANS vapor at about 550 K. Maximum fluorescence intensity is obtained at an excitation wavelength of 336 nm (∼3.7 eV). The experimental observation of an increase of the excitation energy in going from DCS to DANS is not reproduced by calculations: INDO/MRD-CI calculations give a value of 3.68 eV for the vertical excitation energy of DANS,[2,3] and CNDO/S calculations give 3.49 eV.[26]

Figure 4 shows that, compared to DCS, many more vibronic transitions have a significant intensity. We believe that this is partly due to saturation effects. Because the vapor pressure of DANS under the present experimental conditions is lower than for DCS, higher laser intensities needed to be used to get an acceptable signal. This is one of the reasons why the resonances in the spectrum of jet-cooled DANS are considerably more difficult to assign and, in fact, cannot be analyzed to the same extent as was done for DCS. In the excitation spectrum of DCS, two relatively strong bands were observed at 14.5 and 22.8 cm^{-1}. Their intensity dependence on temperature and expansion conditions gave us reason to believe that they should be assigned as hot bands. In the excitation spectrum of DANS, we observe two strong lines at 23.1 and 27.1 cm^{-1} that we assign similarly. As might be expected, many of the higher-lying transitions show combination bands with these two transitions, which is another reason it is so difficult to come to a complete assignment.

To extract nevertheless useful spectroscopic information on S_1 from the spectrum, we will in the first instance assume that the geometry changes occurring upon excitation are similar in DCS and DANS and, thus, that a similar Franck−Condon pattern may be expected for the two compounds. On the basis of this assumption, we observe a shift between DCS and DANS for certain features in the fluorescence excitation spectrum. For DCS, we have seen that the dominant modes involve principally

(combinations of) modes of the *trans*-stilbene backbone. The observed shifts might then be interpreted as resulting from a difference of the electronic character of the first excited state of DCS and DANS because of a difference in the push−pull strength for the two compounds. Brédas et al.[2] have calculated the π bond-order modifications in DANS upon excitation from S_0 to S_1. Particularly in the ethylene part of the *trans*-stilbene backbone, a strong reversal in the π bond order is predicted. It is conceivable that these π bond-order changes upon excitation are more pronounced for DANS than for DCS, because the increase of the dipole moment, i.e., the push−pull strength, of DANS upon $S_1 \leftarrow S_0$ excitation is noticeably larger than for DCS.[26]

Table 3 presents a summary of the vibrational frequencies of the optically active low-frequency vibrational modes of the stilbene backbone in DANS. On the basis of our experience with DCS, we expect a′(2) to be one of the most active modes in DANS and we expect its ν_{25}-character partner a′(3) to be present as well. In this spirit, we assign the very intense line at 155.1 cm^{-1} as the $a'(2)_0^1$ transition in DANS. An overtone of this transition is observed at 310.8 cm^{-1}. The corresponding blue shift of 26.2 cm^{-1} for this transition in DANS might be taken as evidence for a stronger π bond-order change in DANS than in DCS. The a′(3) transition is more difficult to find: the resonance at 141.9 cm^{-1} might apply, and indeed, its combination with the 155 cm^{-1} line is easily found, but such an assignment would imply a red shift of 27.2 cm^{-1} with respect to DCS, and for the ground state of the two compounds, such a decrease is not predicted (see Table 1). The strong line at 205.5 cm^{-1} is assigned to the same transition as the feature at 201.2 cm^{-1} for DCS, i.e., the $a'(4)_0^1$ transition. The small difference in frequency indicates that this mode has not much been affected by the π bond-order modification in the ethylene part of DANS upon excitation.

Similar to the fluorescence excitation spectrum of jet-cooled DCS, we observe a line at 49.2 cm^{-1} in the spectrum of DANS, which is assigned to the $a''(3)_0^2$ transition. More difficult is the assignment of the two-quanta transition of the other out-of-plane mode active in DCS, $a''(2)_0^2$, because there is no feature at ∼89 cm^{-1} with a similar intensity as the feature at 89.4 cm^{-1} in the spectrum of DCS. It is conceivable that the ν_{37} mode of *trans*-stilbene is affected by the stronger π bond-order modifications upon excitation in DANS than in DCS. This could lead to a blue shift of the vibrational frequency of this mode because the π bond order of the C_e−Ph bond in DANS will show a larger increase than in DCS. We believe that the feature at 105.4 cm^{-1} in the fluorescence excitation spectrum of DANS is related to the line at 89.4 cm^{-1} in the spectrum of DCS and assign it therefore as the $a''(2)_0^2$ transition. This assignment is supported by the expected presence of a strong feature at 77.5 cm^{-1}, which can be readily assigned as the $a''(2)_0^1 a''(3)_0^1$ transition. In DCS, some relatively strong features could be observed in the high-energy part of the spectrum. This is also observed for DANS, but less pronounced. In fact, the modes that we can assign in this case, in part because of the presence of some combination bands, are the $a'(12)_0^1$, $a'(13)_0^1$, and $a'(15)_0^1$ transitions at 593.4, 615.3, and 736.7 cm^{-1}.

The fluorescence excitation spectra of DCS (Figure 2) and DANS (Figure 4) extend both to about 800 cm^{-1} above the 0−0 transition. Fluorescence decay measurements as a function of the excess vibrational energy in isolated DCS[50] have revealed that the fluorescence lifetimes are constant up to about an excess energy of 750 cm^{-1} (2.1 kcal/mol), after which they decrease rapidly. This is in line with the presence of a competitive, nonradiative, relaxation pathway, attributed to cis ← trans photoisomerization. For DCS, this photoisomerization has been studied extensively as a function of solvent polarity.[14,16,17,24,25] In an apolar solvent such as *n*-heptane, the activation energy for cis ← trans photoisomerization of DCS has been determined to be about 3.3 kcal/mol.[24] The activation energy increases strongly with solvent polarity, reflecting the idea[16] that the transition state is less polar than the LE state, or possibly the CT state,[24] and will consequently be less stabilized in the condensed phase. Görner has determined that for DANS the activation energy in an apolar solvent like *n*-pentane is about 4.3 kcal/mol,[34] i.e., somewhat higher than for DCS, which is in line with the larger dipole moment of the equilibrated singlet excited state of DANS. However, the present study shows that under isolated conditions both push−pull stilbenes have a similar activation barrier. This implies that the larger value of the activation barrier found for DANS in an apolar solvent is predominantly due to solute−solvent interactions, or vice versa, that solute−solvent interactions have a larger influence on the spectroscopy of DANS than of DCS. This will be confirmed when excitation energies measured in solvents will be compared with the gas-phase ones (section E).

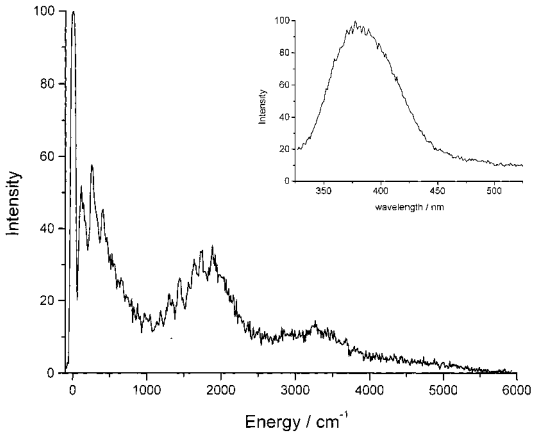

Figure 5. Emission spectrum of jet-cooled DANS excited at the 0−0 transition (28 200.1 cm^{-1}) to the first excited singlet state. Fluorescence wavelengths are given as shifts from the excitation wavelength. The inset displays the emission spectrum of DANS vapor at 550 K (λ_{exc}=340 nm).

Figure 5 shows the dispersed fluorescence emission spectrum taken at the 0_0^0 $S_1(2^1A') \leftarrow S_0(1^1A')$ transition in DANS, heated to about 470 K and seeded in a supersonic jet expansion of He. The contour of the spectrum strongly resembles that of the dispersed emission spectrum of jet-cooled DCS (Figure 3). Again, because of the poor resolution, we will not embark on any assignments of the ground state frequencies of DANS but only notice that similar to DCS low-frequency modes and modes around 1200−1300 and 1600 cm^{-1} are dominantly active. The fluorescence emission spectrum of a heated quartz cell containing DANS vapor at 550 K has been depicted in the inset of Figure 5. Under these conditions, maximum fluorescence intensity is collected at 369 nm (∼27 100 cm^{-1}).

Previously, efforts to simulate the one-photon absorption (OPA) and two-photon absorption (TPA) spectra and the third-harmonic generation (THG) frequency dependent curve of a side-chain polymer containing DANS as its side group did not succeed in reproducing the red shift measured between linear and nonlinear spectra.[2] To properly account for this red shift, a displaced oscillators model was set up using two displacement factors b_i of 1.7 and 1.1, associated with the C═C stretching mode within the vinylene linkage, and the breathing mode of

the phenylene rings, respectively. Our experiments on DANS and DCS can put these results into a somewhat more detailed perspective. Displacement factors can in general be determined reliably from excitation as well as emission spectra.[71,72] In the present case, however, the molecules under investigation are subject to a radiationless process in the excited state, which is dependent on the excess vibrational energy. As a result, the measured intensities in the excitation spectrum do not only depend on the vibrational overlap integrals from which the displacement factors would be determined. We will restrict us therefore to a discussion of what the emission spectra, which do not suffer from this drawback, can tell us. First, in an emission spectrum the intensity ratio $(\nu_i)_1^0/0_0^0$ is equal to $b_i^2/2$; one needs to be careful, however, of the influence of normal mode rotations, as is amply clear from theoretical studies on *para*-phenylenevinylenes.[68,73] Nevertheless, under the assumed conditions of the absence of Duschinski rotations and the conservation of vibrational frequencies upon excitation,[2] the gas-phase experiments on substituted stilbenes would favor smaller values for the displacement factors, roughly 0.9 and 0.6, respectively. Second, the excitation and emission spectra indicate that, apart from the two previously mentioned modes, one or more low-frequency modes would also need to be taken into account. This conclusion is supported by previous calculations on *trans*-stilbene,[68] which predict a large displacement factor for ν_{25}.

D. 4-Di(hydroxy-ethyl)amino-4′-nitrostilbene (DANS-diol). So far we have considered two molecular systems that are of interest to us because of their nonlinear optical properties and their associated potential use in, for example, second-harmonic generators and optoelectronic devices. From the point of view of actual application, these compounds are still rather idealized, because under applicative circumstances they are employed in a chemically different form, for example, as a side group in a side-chain polymer as described above. It is therefore of interest to consider a chemical form of the chromophore that resembles more closely the one employed in an application, although one does not expect that the (non)linear optical properties in this form differ dramatically from the "idealised" forms considered so far. To this purpose, we have tried and investigated DANS-diol. The one-photon fluorescence excitation spectrum of the $S_1(2^1A') \leftarrow S_0(1^1A')$ transition of this compound, heated to about 490 K and seeded in an expansion of He, is shown in Figure 6. The inset of Figure 6 presents the low-resolution fluorescence excitation spectrum of DANS-diol vapor in a quartz cell at 550 K. Maximum fluorescence intensity is obtained here at an excitation wavelength of 337 nm ($\sim$29 670 cm^{-1}). We notice that also for this molecule the gas-phase excitation energy is higher than for DCS, whereas the excitation energy in low-polarity solvents is lower than for DCS.

Because the two hydroxy-ethyl groups can adopt various conformations in the amino donor group that are expected to be close in energy, one may anticipate a complicated spectrum arising from the superposition of the excitation spectra of several conformers of DANS-diol. Changing the expansion conditions indeed results in an increase of the relative intensities of the features in the low-energy region with respect to the strong line at 28 793.3 cm^{-1} and other features in the high-energy region of the spectrum. Although the presence of more than one conformer complicates to a certain extent the assignment of the various resonances, the possibility to obtain excitation spectra under different temperature conditions enables us to group resonances that belong to one particular conformation.

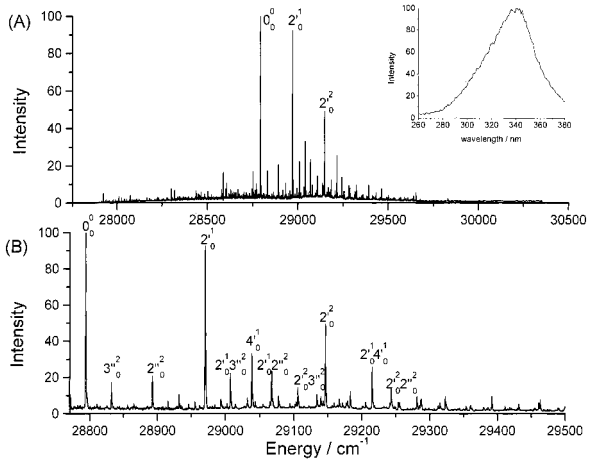

Figure 6. Fluorescence excitation spectrum of the $S_1 \leftarrow S_0$ transition of jet-cooled DANS-diol. The spectrum shows the superposition of excitation spectra of several conformers of DANS-diol. The most intense feature at 28 793.3 cm^{-1} is assigned as the 0−0 transition of the most abundant conformer. (A) Overall $S_1 \leftarrow S_0$ excitation spectrum. The inset displays the excitation spectrum of DANS-diol vapor at 550 K. (B) Expanded view of the 28 800−29 500 cm^{-1} region.

TABLE 4: Assignments of the Vibronic Transitions in the $S_1(2^1A') \leftarrow S_0(1^1A')$ Fluorescence Excitation Spectrum of Jet-Cooled DANS-diol[a]

energy	intensity	assignment	energy	intensity	assignment
0	100	0_0^0	460.1	4	$2'^1_0 4'^1_0 3''^2_0$
38.6	17	$3''^2_0$	487.6	7	$2'^2_0 2''^2_0 3''^2_0$
99.1	21	$2''^2_0$	491.0	3	$4'^2_0$
138.1	9	$2''^2_0 3''^2_0$	521.3	4	$2'^1_0 4'^1_0 2''^2_0$
176.4	100	$2'^1_0$	529.4	8	$2'^3_0$
213.8	21	$2'^1_0 3''^2_0$	560.0	2	$2'^1_0 4'^1_0 2''^2_0 3''^2_0$
245.2	30	$4'^1_0$	568.5	2	$2'^1_0 3''^2_0$
274.3	21	$2'^1_0 2''^2_0$	598.0	8	$2'^2_0 4'^1_0$
284.3	7	$4'^1_0 3''^2_0$	627.0	2	$2'^3_0 2''^2_0$
313.8	3	$2'^1_0 2''^2_0 3''^2_0$	667.3	5	$2'^1_0 4'^2_0$
346.1	6	$4'^1_0 2''^2_0$	667.9	2	$2'^3_0 2''^2_0 3''^2_0$
352.7	47	$2'^2_0$	706.4	3	$2'^4_0$
383.6	3	$4'^1_0 2''^2_0 3''^2_0$	774.1	2	$2'^3_0 4'^1_0$
389.7	11	$2'^2_0 3''^2_0$	845.0	3	$2'^2_0 4'^2_0$
421.7	23	$2'^1_0 4'^1_0$	882.2	1	$2'^5_0$
449.5	11	$2'^2_0 2''^2_0$			

[a] The assignments are those for the most abundant conformer of DANS-diol with its 0−0 transition at 28 793.3 cm^{-1}.

The feature at 28 793.3 cm^{-1} in the fluorescence excitation spectrum is assigned as the 0−0 transition of the most abundant conformer. This resonance will be used as a reference to determine the assignments of the vibronic transitions in this conformer and, thus, the vibrational frequencies in the excited state. In contrast with the difficulties encountered when trying to assign the various resonances in the fluorescence excitation spectrum of DANS, we find here that the majority of the strong lines can be readily assigned as overtones and/or combination bands of four modes. Because we have not performed ab initio calculations of the harmonic force field of the electronic ground state of this molecule, we stick to the nomenclature of the modes in DCS and DANS. In Table 3, the frequencies of these modes are reported, whereas Table 4 summarizes the vibrational assignments of the resonances in the excitation spectrum of jet-cooled DANS-diol.

The strong resonances at 38.6 and 99.1 cm^{-1} are assigned as the $a''(2)_0^2$ and $a''(3)_0^2$ transitions, related to the 36_0^2 and 37_0^2 transitions in *trans*-stilbene, respectively. In agreement with an

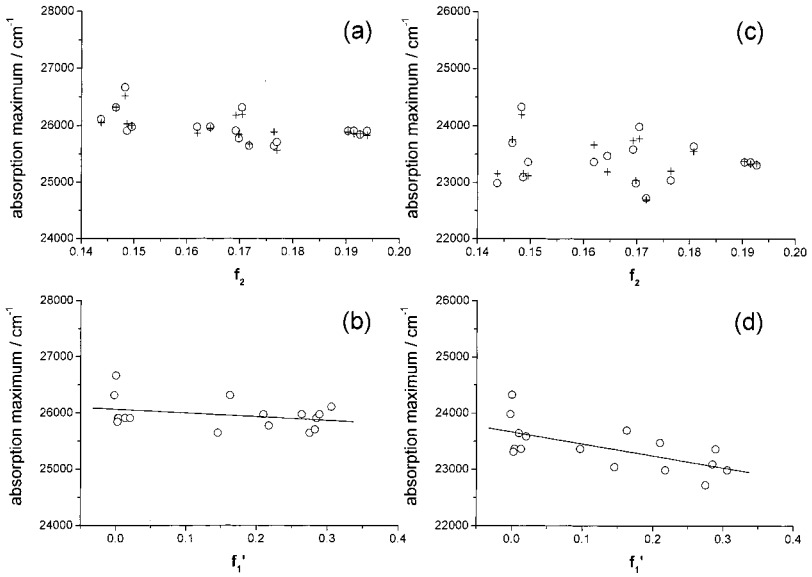

Figure 7. Fits of the absorption maxima of DCS (a and b) and DANS (c and d). Fits a and c concern three-parameter fits using the McRae-Bayliss model for solvatochroism (eq 1), and b and d concern two-parameter fits using the Onsager formulizm (eq 2). The experimentally determined maxima are indicated with circles, and the fitted values in a and c are indicated with a +.

expected red shift that is due to substitution of the methyl groups with hydroxy-ethyl side chains, this implies a pronounced red shift of 10.6 and 6.3 cm^{-1}, respectively, for these modes in DANS-diol with respect to DANS. The $a'(4)_0^1$ transition in DANS-diol is assigned to an intense line at 245.2 cm^{-1}, with an overtone visible at 491.0 cm^{-1}. The most active vibration in the excitation spectrum is a′(2). The $a'(2)_0^1$ transition is the very intense feature at 176.4 cm^{-1}, and a relatively long progression is observed for this mode: the $a'(2)_0^2$ transition occurs at 352.7 cm^{-1}, $a'(2)_0^3$ at 529.4 cm^{-1}, $a'(2)_0^4$ at 706.4 cm^{-1}, and $a'(2)_0^5$ at 882.2 cm^{-1}. This long progression is actually somewhat surprising, considering that in DCS and DANS only the first overtone was seen, and might in principle either indicate that for this form of the DANS chromophore larger geometry changes occur upon excitation or that the lifetime of the higher vibrational levels in DANS-diol does not decrease as rapidly as for DCS or DANS. Direct measurements of the fluorescence lifetimes in DCS[50] have shown that up to about 750 cm^{-1} the excited state lifetime hardly changes and would therefore favor the former possibility. In the previous section, it was noticed that for a proper simulation of the OPA and TPA spectra and the THG frequency dependent curve[2] it was required to take the geometry changes occurring upon excitation into account. The observation of a longer progression for the a′(2) mode in DANS-diol than in DANS or DCS thus also implies that the nonlinear optical properties of the DANS chromophore might be more affected in DANS-diol than one would intuitively expect.

E. Solvent Dependence. In the previous sections, we have investigated the spectroscopic properties of push−pull stilbenes under isolated conditions and considered the influence of a slight chemical modification as a first step toward understanding their properties when actually used in applications. Armed with this knowledge, it is now of interest to make another step toward their applicative use by considering the influence of interactions of the chromophores with their surroundings. To this purpose, the present data will be confronted with spectroscopic data obtained in various solvents. Assuming that the interaction of the electronic ground state and the lowest excited singlet state of DCS and DANS with the solvent can be described as that of a point dipole occupying a spherical cavity in a dielectric continuum characterized by its dielectric constant ϵ and refractive index n, we can apply the McRae−Bayliss model for solvatochroism[74−77] to analyze the available data. This model contains two variables, f_1 and f_2, which are functions of the dielectric constant ϵ and the refractive index n of the solvent:

$$\tilde{\nu} = \tilde{\nu}_0 + Af_1 + Bf_2$$

$$f_1 = \frac{\epsilon - 1}{\epsilon + 2} - \frac{n^2 - 1}{n^2 + 2}$$

$$f_2 = \frac{n^2 - 1}{2n^2 + 1} \qquad (1)$$

in which $\tilde{\nu}_0$ is the transition energy in the gas phase. The A term derives from the electrostatic forces between solute and solvent and gives rise to the so-called reorganizational or nuclear polarization factor, and the B term involves the solute dipole−solvent polarizability interactions and gives rise to the electronic polarization factor. Previously, the solvation dependence of spectroscopic data of DCS has been analyzed employing a simpler approach,[24] taking only the nuclear polarization factor f_1 into account, as is usual practice for polar molecules such as these where large changes in dipole moment upon excitation occur. In that case, however, the Onsager form was employed:

$$f'_1 = \frac{\epsilon - 1}{2\epsilon + 1} - \frac{n^2 - 1}{2n^2 + 1} \qquad (2)$$

For comparison we will therefore present in the following also fits based on a f'_1 dependence only.

Figure 7 displays the results of these fits of the absorption data reported by Gruen et al.[13,27] to eqs 1 and 2, whereas the parameters that follow from the fits are given in Table 5. When we first consider the data for DCS, Figure 7 parts a and b clearly show that the quality of the fit is significantly improved when the electronic polarization factor is taken into account. The parameters obtained from these fits demonstrate that the electronic polarization factor dominates by far the spectral shift occurring in going from gas to solvent. On the other hand, for the solvents considered here, this term is more or less constant,

TABLE 5: Results of Fits of Absorption Data of DCS and DANS in Solution to Equations 1 and 2

	$\tilde{\nu}_0/10^3$ cm^{-1}	$A/10^3$ cm^{-1}	$B/10^3$ cm^{-1}
DCS[a]	28.7 (0.4)	−0.75 (0.13)	−14.9 (2.3)
DCS[b]	26.1 (0.1)	−0.66 (0.50)	
DANS[a]	27.0 (0.6)	−1.58 (0.20)	−19.1 (3.3)
DANS[b]	23.7 (0.1)	−2.12 (0.67)	

[a] Fit to eq 1. [b] Fit to eq 2.

and the differences between the various solvents are dominated by the nuclear polarization term. Although, of course, the three-parameter fit performs significantly better, both fits lead to values for the gas-phase excitation energy that are in line with the value obtained in the present study for the 0−0 transition (27 061 cm^{-1}) and the maximum in the absorption spectrum of DCS vapor (28 410 cm^{-1}).

This situation changes dramatically when fits of the DANS data are considered (Figure 7 parts c and d). Although here the electronic polarization factor once again dominates the absolute value of the solvent shift, the nuclear polarization factor plays a considerably larger role. Moreover, we see that application of the simple model of eq 2 leads to a value for the gas-phase excitation energy (23 700 cm^{-1}) that is way off from the experimental values for the 0−0 transition (28 200 cm^{-1}) and the maximum in the absorption spectrum of DANS vapor (29 760 cm^{-1}). As a result, the simple rule of thumb that excitation energies in nonpolar solvents give a reasonable idea of the excitation energy in the gas-phase that was seen to hold so nicely for DCS is not valid for DANS. The extrapolated value obtained from the three-parameter fit comes much closer to the gas-phase data but still not as good as that for DCS.

One might speculate about the reason for the observed difference between the solvation behavior of the two compounds. In principle, the employed description of solute−solvent interactions (partly) might fail in the case of DANS. This then would imply that we cannot consider the solvated molecule as a molecule in a dielectric continuum, but that solute and one or more solvent molecules should be treated as one molecular system. Alternatively, the dissimilarity might be caused by changes in the electronic structure of DANS upon solvation, which might be translated into significant changes of the geometry in ground and excited states with respect to the gas phase.

IV. Summary and Conclusions

We have shown that the high-resolution fluorescence excitation spectra of the $S_1(2^1A') \leftarrow S_0(1^1A')$ transition in jet-cooled DCS and DANS can be well assigned on the basis of ab initio B3LYP/6-31G* calculations of the harmonic force fields of the electronic ground state of *trans*-stilbene, DCS, and DANS. The excitation spectrum of both push−pull stilbenes is dominated by vibronic transitions involving vibrational modes of the stilbene-like backbone. However, a characterization in terms of *trans*-stilbene vibrational terminology has to be done with caution because of the absence of a clear one-to-one correspondence between the substituted stilbenes and *trans*-stilbene.

The strong and efficient charge-transfer in these push−pull stilbenes, resulting in a significant enhancement of the nonlinear optical response, has put DANS in the role of a benchmark system for the development of an appropriate theoretical model describing this response. The present study has provided new information necessary to set up such a model, showing, for example, that displacement factors utilized previously may well have been overestimated and suggesting that one or more low-frequency modes should be taken into account.

Comparison of the spectroscopic data of the DANS chromophore in DANS and DANS-diol has shown that this auxiliary function has a significant effect on its spectroscopic properties. The fluorescence excitation spectra of DANS and DCS demonstrate that for these molecules an efficient nonradiative relaxation pathway attributed to cis ← trans photoisomerization becomes important for excess vibrational energies of about 800 cm^{-1} in S_1. The fluorescence excitation spectrum of jet-cooled DANS-diol extends significantly further, thereby suggesting that the activation barrier in the gas-phase for this photoreaction in DANS-diol is significantly larger. Moreover, the observation of a longer progression in DANS-diol for the a′(2) mode than in DANS or DCS implies as well that the nonlinear optical properties of the DANS chromophore could be more affected in DANS-diol than one would intuitively expect.

Finally, the present study has shown that spectroscopic data obtained in solution for DCS are smoothly linked to the gas-phase data. For DANS and DANS-diol, in contrast, we are led to the conclusion that solute−solvent interactions play a dominant role already for low-polarity solvents. This conclusion finds additional support in the observation that in the gas-phase both compounds have a similar activation barrier for cis ← trans photoisomerization, whereas upon solvation in apolar solvents, this barrier increases significantly more for DANS than for DCS. In this respect, it would be interesting to study the effect of solute−solvent interactions on the fluorescence excitation spectrum of photoexcited DCS and DANS seeded in a supersonic jet expansion as small clusters with solvent molecules ranging from apolar to polar. Such experiments are presently in progress.

To extend the spectroscopic information needed to model and predict the nonlinear optical response of compounds such as DANS, it would be highly rewarding to study selectively bridged derivatives of DANS in which the nonradiative cis ← trans photoisomerization pathway is blocked. In this way, the measured vibronic line intensities in the excitation spectrum would be mainly dominated by the vibrational overlap integrals and not be influenced by nonradiative relaxation, which, in turn, would allow an accurate determination of the displacement factors of those vibrational modes that are crucial for an accurate evaluation of the nonlinear optical response. Moreover, under the applicative conditions in which DANS is incorporated via covalent linking in a side-chain polymer, cis ← trans photoisomerization has been shown to be slowed considerably, suggesting that the photophysics and photochemistry of a selectively bridged DANS derivative blocking this nonradiative relaxation channel would more closely resemble those of DANS incorporated in a polymeric environment. A final point of interest concerns the spectroscopic properties of higher excited singlet states, because the nonlinear optical response is also determined by contributions from these states. For DANS, for example, it has been found that S_2 should also be incorporated in a theoretical model to account for the low-energy optical response. To this purpose resonance enhanced multiphoton ionization photoelectron spectroscopy (REMPI−PES) will be employed soon. This experimental technique will not only enable us to probe higher excited singlet states but also to project the excited-state wave function of S_1, after photoexcitation from S_0, onto S_2 and possibly other higher singlet excited states by two-color experiments.

Acknowledgment. Part of this work has been supported by the European Community (TMR Contract No. ERBFMRX-CT970097). The authors thank R. Sitters and J. Scheijde for

technical support and Prof. J. W. Verhoeven and Prof. C. A. de Lange for use of equipment.

References and Notes

(1) *Chem. Rev.* **1994**, *94*, special issue on *Optical Nonlinearities in Chemistry*.
(2) Beljonne, D.; Brédas, J.-L.; Cha, M.; Torruellas, W. E.; Stegeman, G. I.; Hofstraat, J. W.; Horsthuis, W. H. G.; Möhlmann, G. R. *J. Chem. Phys.* **1995**, *103*, 7834.
(3) Beljonne, D.; Brédas, J.-L.; Chen, G.; Mukamel, S. *Chem. Phys.* **1996**, *210*, 353.
(4) Williams, D. J.; Prasad, P. *Introduction to Nonlinear Optical Effects in Molecules and Polymers*; John Wiley & Sons: New York, 1991.
(5) Brédas, J.-L.; Chance, R. R. *Conjugated Polymeric Materials: Opportunities in Electronics, Optoelectronics, and Molecular Electronics*; NATO-ARW Series E182; Kluwer: Dordrecht, The Netherlands, 1990.
(6) Messier, J.; Kajzar, F.; Prasad, P. *Organic Molecules for Nonlinear Optics and Photonics*; NATO-ARW Series E194; Kluwer: Dordrecht, The Netherlands, 1991.
(7) Albota, M.; Beljonne, D.; Brédas, J.-L.; Ehrlich, J. E.; Fu, J.-Y.; Heikal, A. A.; Hess, S. E.; Kogej, T.; Levin, M. D.; Marder, S. R.; McCord-Maughon, D.; Perry, J. W.; Röckel, H.; Rumi, M.; Subramaniam, G.; Webb, W. W.; Wu, X.-L.; Xu, C. *Science* **1998**, *281*, 1653.
(8) Cumpston, B. H.; Ananthavel, S. P.; Barlow, S.; Dyer, D. L.; Ehrlich, J. E.; Erskine, L. L.; Heikal, A. A.; Kuebler, S. M.; Lee, I.-Y. S.; McCord-Maughon, D.; Qin, J.; Röckel, H.; Rumim, M.; Wu, X.-L.; Marder, S. R.; Perry, J. W. *Nature* **1999**, *398*, 51.
(9) Marder, S. R.; Gorman, C. B.; Meyers, F.; Perry, J. W.; Bourhil, G.; Brédas, J.-L.; Pierce, B. M. *Science* **1994**, *265*, 632.
(10) Meyers, F.; Marder, S. R.; Pierce, B. M.; Brédas, J.-L. *J. Am. Chem. Soc.* **1994**, *116*, 10703.
(11) Meyers, F.; Marder, S. R.; Pierce, B. M.; Brédas, J.-L. *Chem. Phys. Lett.* **1994**, *228*, 171.
(12) Mukamel, S.; Takahashi, A.; Wang, H. X.; Chen, G. *Science* **1994**, *266*, 250.
(13) Gruen, H.; Görner, H. *Z. Naturforsch. A* **1983**, *38*, 928.
(14) Lapouyade, R.; Czeschka, K.; Majenz, W.; Rettig, W.; Gilabert, E.; Rullière, C. *J. Phys. Chem.* **1992**, *96*, 9643.
(15) Létard, J.-F.; Lapouyade, R.; Rettig, W. *J. Am. Chem. Soc.* **1993**, *115*, 2441.
(16) Rettig, W.; Majenz, W.; Herter, R.; Létard, J.-F.; Lapouyade, R. *Pure Appl. Chem.* **1993**, *65*, 1699.
(17) Rettig, W.; Strehmel, B.; Majenz, W. *Chem. Phys.* **1993**, *173*, 525.
(18) Gilabert, E.; Lapouyade, R.; Rullière, C. *Chem. Phys. Lett.* **1988**, *145*, 262.
(19) Gilabert, E.; Lapouyade, R.; Rullière, C. *Chem. Phys. Lett.* **1991**, *185*, 82.
(20) Abraham, E.; Oberlé, J.; Jonusauskas, G.; Lapouyade, R.; Rullière, C. *Chem. Phys.* **1997**, *214*, 409.
(21) Abraham, E.; Oberlé, J.; Jonusauskas, G.; Lapouyade, R.; Rullière, C. *Chem. Phys.* **1997**, *219*, 73.
(22) Rettig, W.; Gilabert, E.; Rullière, C. *Chem. Phys. Lett.* **1994**, *229*, 127.
(23) Eilers-König, N.; Kühne, T.; Schwarzer, D.; Vöhringer, P.; Schroeder, J. *Chem. Phys. Lett.* **1996**, *253*, 69.
(24) Il'ichev, Y. V.; Kühnle, W.; Zachariasse, K. *Chem. Phys.* **1996**, *211*, 441.
(25) Rettig, W.; Majenz, W.; Lapouyade, R.; Vogel, M. *J. Photochem. Photobiol. A: Chem.* **1992**, *65*, 95.
(26) Lapouyade, R.; Kuhn, A.; Létard, J.-F.; Rettig, W. *Chem. Phys. Lett.* **1993**, *208*, 48.
(27) Gruen, H.; Görner, H. *J. Phys. Chem.* **1989**, *93*, 7144.
(28) Gegiou, D.; Muszkat, K. A.; Fischer, E. *J. Am. Chem. Soc.* **1968**, *90*, 3907.
(29) Schulte-Frohlinde, D.; Blume, H.; Güsten, H. *J. Phys. Chem.* **1962**, *66*, 2486.
(30) Bent, D. V.; Schulte-Frohlinde, D. *J. Phys. Chem.* **1974**, *78*, 446.
(31) Bent, D. V.; Schulte-Frohlinde, D. *J. Phys. Chem.* **1974**, *78*, 451.
(32) Gruen, H.; Schulte-Frohlinde, D. *J. Photochem.* **1978**, *8*, 91.
(33) Schulte-Frohlinde, D.; Gruen, H. *Pure Appl. Chem.* **1979**, *51*, 279.
(34) Görner, H. *J. Photochem. Photobiol. A: Chem* **1987**, *40*, 325.
(35) de Haas, M. P.; Warman, J. M. *Chem. Phys.* **1982**, *73*, 35.
(36) Warman, J. M.; de Haas, M. P.; Hummel, A.; Varma, C. A. G. O.; Zeyl, H. M. *Chem. Phys. Lett.* **1982**, *87*, 83.
(37) Salem, L. *Acc. Chem. Res.* **1979**, *12*, 87.
(38) Dauben, W. G.; Ritscher, J. S. *J. Am. Chem. Soc.* **1970**, *92*, 2925.
(39) Wulfman, C. E.; Kumei, S. E. *Science* **1971**, *172*, 1061.
(40) Albert, I. D. L.; Ramasesha, S. *J. Phys. Chem.* **1990**, *94*, 6540.
(41) Smirnov, S. N.; Braun, C. L. *Chem. Phys. Lett.* **1994**, *217*, 167.
(42) Kawski, A.; Gryczynski, I.; Jung, Ch.; Heckner, K.-H. *Z. Naturforsch. A* **1977**, *32*, 420.
(43) Gryczynski, I.; Gloyna, D.; Kawski, A. *Z. Naturforsch. A* **1980**, *35*, 777.
(44) Liptay, W. *Excited States*; Academic Press: New York, 1974; Volume 1.
(45) Czekella, J.; Liptay, W.; Meyer, K.-O. *Ber. Bunsen-Ges. Phys. Chem.* **1963**, *67*, 465.
(46) Lippert, E. *Z. Elektrochem.* **1957**, *61*, 962.
(47) Moll, F.; Lippert, E. *Z. Elektrochem.* **1954**, *58*, 853.
(48) Amatatsu, Y. *Theor. Chem. Acc.* **2000**, *103*, 445.
(49) Flipse, M. C.; de Jong, R.; Woudenberg, R. H.; Marsman, A. W.; van Walree, C. A.; Jenneskens, L. W. *Chem. Phys. Lett.* **1995**, *245*, 297.
(50) Daum, R.; Hansson, T.; Nörenberg, R.; Schwarzer, D.; Schroeder, J. *Chem. Phys. Lett.* **1995**, *246*, 607.
(51) Williams, R. M.; Koeberg, M.; Lawson, J. M.; An, Y.-Z.; Rubin, Y.; Paddon-Row, M. N.; Verhoeven, J. W. *J. Org. Chem.* **1996**, *61*, 5055.
(52) Zwier, J. M.; Brouwer, A. M.; Rijkenberg, R. A.; Buma, W. J. *J. Phys. Chem. A* **2000**, *104*, 729.
(53) Rijkenberg, R. A.; Bebelaar, D.; Buma, W. J. *J. Am. Chem. Soc.* **2000**, *122*, 7418.
(54) Frisch, M. J.; Trucks, G. W.; Schlegel, H. B.; Scuseria, G. E.; Robb, M. A.; Cheeseman, J. R.; Zakrzewski, V. G.; Montgomery, J. A., Jr.; Stratmann, R. E.; Burant, J. C.; Dapprich, S.; Millam, J. M.; Daniels, A. D.; Kudin, K. N.; Strain, M. C.; Farkas, O.; Tomasi, J.; Barone, V.; Cossi, M.; Cammi, R.; Mennucci, B.; Pomelli, C.; Adamo, C.; Clifford, S.; Ochterski, J.; Petersson, G. A.; Ayala, P. Y.; Cui, Q.; Morokuma, K.; Malick, D. K.; Rabuck, A. D.; Raghavachari, K.; Foresman, J. B.; Cioslowski, J.; Ortiz, J. V.; Stefanov, B. B.; Liu, G.; Liashenko, A.; Piskorz, P.; Komaromi, I.; Gomperts, R.; Martin, R. L.; Fox, D. J.; Keith, T.; Al-Laham, M. A.; Peng, C. Y.; Nanayakkara, A.; Gonzalez, C.; Challacombe, M.; Gill, P. M. W.; Johnson, B. G.; Chen, W.; Wong, M. W.; Andres, J. L.; Head-Gordon, M.; Replogle, E. S.; Pople, J. A. *Gaussian 98*, revision A.7; Gaussian, Inc.: Pittsburgh, PA, 1998.
(55) Becke, A. D. *J. Chem. Phys.* **1993**, *98*, 5648.
(56) Spangler, L. H.; Bosma, W. B.; van Zee, R. D.; Zwier, T. S. *J. Chem. Phys.* **1988**, *88*, 6768.
(57) Yan, S.; Spangler, L. H. *J. Phys. Chem.* **1995**, *99*, 3047.
(58) Siewert, S.; Spangler, L. H. *J. Phys. Chem.* **1995**, *99*, 9316.
(59) Metzger, B. S.; Spangler, L. H. *J. Phys. Chem. A* **1997**, *101*, 5431.
(60) Spangler, L. H.; van Zee, R.; Zwier, T. S. *J. Phys. Chem.* **1987**, *91*, 2782.
(61) Syage, J. A.; Felker, P. M.; Zewail, A. H. *J. Chem. Phys.* **1984**, *81*, 4685.
(62) Chiang, W.-Y.; Laane, J. *J. Chem. Phys.* **1994**, *100*, 8755.
(63) Truett, J.; Uzi, E.; Jortner, J. *J. Chem. Phys.* **1984**, *81*, 2330.
(64) Takahashi, M.; Kimura, K. *J. Phys. Chem.* **1995**, *99*, 1628.
(65) Champagne, B. B.; Pfanstiel, J. F.; Plusquellic, D. F.; Pratt, D. W.; van Herpen, W. M.; Meerts, W. L. *J. Phys. Chem.* **1990**, *94*, 6.
(66) Meic, Z.; Güsten, H. *Spectrochim. Acta A* **1978**, *34*, 101.
(67) Choi, C. H.; Kertesz, M. *J. Phys. Chem. A* **1997**, *101*, 3823.
(68) Negri, F.; Orlando, G.; Zerbetto, F. *J. Phys. Chem.* **1989**, *93*, 5124.
(69) Palmö, K. *Spectrochim. Acta A* **1988**, *44*, 341.
(70) Grassian, V. H.; Warran, J. A.; Bernstein, E. R.; Secor, H. V. *J. Chem. Phys.* **1989**, *90*, 3994.
(71) Buma, W. J.; Zerbetto, F. *J. Am. Chem. Soc.* **1996**, *118*, 9178.
(72) Zwier, J. M.; Wiering, P. G.; Brouwer, A. M.; Bebelaar, D.; Buma, W. J. *J. Am. Chem. Soc.* **1997**, *119*, 11523.
(73) Karabunarliev, S.; Baumgarten, M.; Bittner, E. R.; Mullen, K. *J. Chem. Phys.* **2000**, *113*, 11372.
(74) Bayliss, N. S.; McRae, E. G. *J. Phys. Chem.* **1954**, *58*, 1002.
(75) McRae, E. G. *J. Phys. Chem.* **1957**, *61*, 562.
(76) McRae, E. G. *Spectrochim. Acta* **1958**, *12*, 192.
(77) Cooper, T. M.; Natarajan, L. V.; Soward, L. A.; Spangler, C. W. *Chem. Phys. Lett.* **1999**, *310*, 508.